Journal of The Physical Society of Japan
Vol. 62, No. 2, February, 1993, pp. 717–730

Magnetic Properties of Extended *t-J* Model. I. Static Properties

Tetsufumi TANAMOTO,* Hiroshi KOHNO and Hidetoshi FUKUYAMA

Department of Physics, Faculty of Science, University of Tokyo, 7-3-1 Hongo, Bunkyo-ku, Tokyo 113

(Received September 16, 1992)

Spin fluctuations in the extended *t-J* model have been investigated within the slave-boson mean-field approximation based on both uniform and singlet RVB states. By choosing the transfer integrals to reproduce the Fermi surface of LSCO and YBCO, we find that incommensurate spin fluctuations can be expected for the Fermi surface of LSCO-type, whereas only commensurate ones for that of YBCO-type, in agreement with experiments. Moreover effects of singlet RVB pairing have been explored and are shown to lead to the qualitative difference of the temperature dependences of the shift of nuclear magnetic resonance in the high and low doping regions as seen experimentally.

§1. Introduction

The nature of spin excitations described by the *t-J* model is of current interest in the context of high-T_c cuprates.[1-4] Although the true ground states and the excitation spectra of the model have been disclosed in rather detail for the one-dimensional case,[5] the studies in two-dimension is far from complete. The mean field theory based on the slave-boson framework, however, together with the fluctuations around the mean-field solutions treated as gauge fields has been shedding interesting and useful insight into this difficult problem. Especially studies on the transport properties based on the uniform resonating-valence-bond (RVB) state and the gauge fluctuations have yielded conclusions compatible with experimental results (semi-)quantitatively or at least qualitatively.[6] Encouraged by this finding the magnetic properties of this uniform RVB state have been explored on the basis of the RPA dynamical susceptibility, $\chi(\boldsymbol{q}, \omega)$, in ref. 7 (referred to as TKF in the following). The main conclusions reached in TKF are as follows:

1) The static uniform susceptibility $\chi \equiv \chi(0, 0)$, which is measured experimentally as the shift, K, of nuclear magnetic resonance (NMR), is almost independent of temperature, T, while at the staggered antiferromagnetic wave vector, $\boldsymbol{Q} \equiv (\pi, \pi)$, $\chi(\boldsymbol{Q}, 0) \equiv \chi_{AF}$ is seen to obey the Curie-Weiß law for a wide range of temperature with a maximum at low temperature.

2) The rate of NMR, $R \equiv (T_1 T)^{-1}$, at the copper (Cu-)site also follows the Curie-Weiß law with a maximum at low temperature. The rate at the oxygen (O-)site is, however, more or less independent of T.

The basic reason why χ_{AF} and R at the Cu-site obey the Curie-Weiß law with a maximum at low temperature is that the $\chi(\boldsymbol{q}, 0)$ has a peak at the commensurate wavevector $\boldsymbol{Q}$ if the temperature is not so low, but that the peak splits into incommensurate peaks as the temperature is lowered. The location of the incommensurate peaks in the Brillouin zone depends on the doping rate, δ.

While these conclusions have explained some of the important features seen in experiments, there remained following serious questions to be addressed;

(A) As has been first stressed by Rice[8] and further explored in ref. 9, there seem to exist qualitative differences in the temperature dependences of R and K between low (L)[10-13] and high (H)[14-16] doping regions as shown in Fig. 1. It is to be noted that Walstedt *et al.*[17]

* Present address: Toshiba R & D center, 1 Komukai Toshiba-cho, Saiwai-ku, Kawasaki 210.

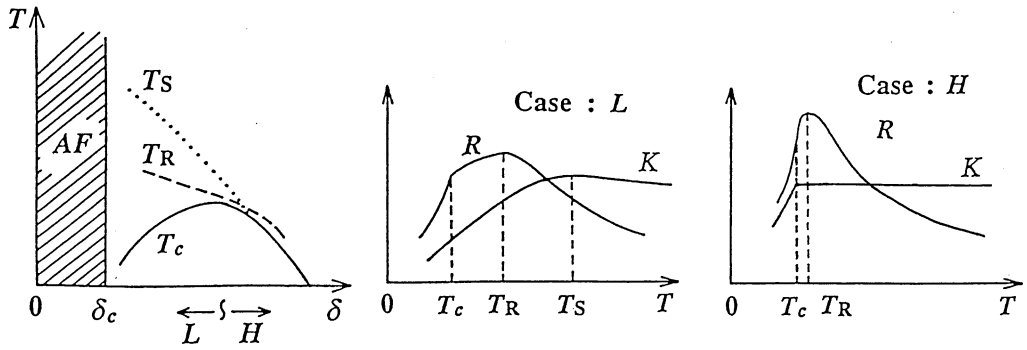

Fig. 1. (a) An experimental magnetic phase diagram on the plane of doping (δ) and temperature (T), with T_c (critical temperature of superconductivity), T_S (onset temperature of the suppression of the spin susceptibility χ), and T_R (the temperature at which NMR rate $(T_1T)^{-1} \equiv R$ takes a maximum). AF indicates the antiferromagnetic phase. There are two characteristic doping regions as seen in the temperature dependences of χ and R which are schematically shown in (b) for low doping (L), and (c) for high doping (H).

observed such qualitative differences in Bi(2212)-compounds between as-grown and annealed samples. Recent experiments by Yoshinari *et al.*[18] indicates that, even in $T_c=90$ K YBCO, T_{RVB} may be located above 20 K higher than T_c. Horvatić *et al.*[19] have actually observed that such qualitative differences are clearly seen in the temperature dependences of $(T_1T)^{-1}$ of even so-called YBCO 90 K samples located very close to the critical concentration giving maximum T_c.

(B) The incommensurate peaks have been observed by the neutron scattering in $La_{2-x}Sr_xCuO_4$ ($x=0.07, 0.14$)[20-24] but not in YBCO,[25-27] where only the commensurate peak is seen.

(C) The existence of the Fermi surfaces in high-T_c cuprates in the doping regions of superconducting phases has been confirmed by the angle-resolved photoemission spectroscopy.[28,29] The actual shapes of the Fermi surfaces are not same among various cuprates,[30-37] which should be incorporated in the study of the magnetic excitations.

We will address ourselves to these questions by extending our former studies into two directions; one is to reflect the shape of the Fermi surface and the other is to show explicitly the qualitative difference between high and low doping. In this paper we examine the static properties deferring the dynamical ones to next papers. A part of the present work has already been reported briefly.[38] We take unit $\hbar = k_B = 1$.

§2. Extended t-J Model and the Fermi Surface

We will study the t-J model on a square lattice and take account of the finite spatial extent of transfer integrals as shown in Fig. 2, while the superexchange interaction is assumed only between the nearest neighbor sites. The reason for this type of the extension of the original t-J model (called extended t-J model in the following) is based on the finding[39-41] that the spatial extent of Zhang-Rice singlet[42] is a sensitive function of the parameters in the original d-p model and the location of the apical oxygens. Especially the transfer in-

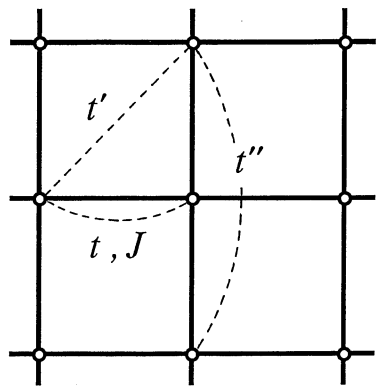

Fig. 2. Transfer integrals of extended range; t (nearest neighbor), t' (next nearest neighbor) and t'' (third neighbor).

tegral between the third neighbors, t'', has been seen to be appreciable as the case may be.[39]

By use of the spinon and holon operators, f_{is} and b_i, introduced *via* the slave-boson formalism, the Hamiltonian is given by

$$H=-\sum_{i,j;s} t_{ij} f_{is}^{\dagger} f_{js} b_j^{\dagger} b_i + \sum_{\langle i,j\rangle} J_{ij} \boldsymbol{S}_i \cdot \boldsymbol{S}_j - \sum_i \lambda_i \left(\sum_s f_{is}^{\dagger} f_{is} + b_i^{\dagger} b_i - 1\right), \tag{2.1}$$

where the transfer integrals up to the third neighbors are taken into account in the first term of the r.h.s. of eq. (2.1) while in the second term the summation is only over the nearest neighbors. The third term represents the local constraint of the total number of spinons and holons being unity at each site. In the following, we fix $t/J=4.0$ and take J as the energy unit, i.e., $J=1$. The lattice spacing is also taken as unity.

In the present mean-field approximation,[43-46] local constraints are loosened to global ones and the Hamiltonian (2.1) is decoupled by introducing two kinds of order parameters, (O_1) $\langle f_{is}^{\dagger} f_{js}\rangle$ and $\langle b_j^{\dagger} b_i\rangle$ representing diagonal coherence of spinons and holons, and (O_2) $\langle f_{is} f_{j-s}\rangle$, or $\langle (f_{i\uparrow} f_{j\downarrow} - f_{i\downarrow} f_{j\uparrow})\rangle/\sqrt{2} \equiv \langle b_{ij}\rangle$ representing singlet pairing of spinons. All of these are in principle dependent on the spatial coordinate. In the uniform RVB state, only (O_1) are finite with translation and spin-rotation invariance. In the singlet RVB state, the off-diagonal order parameter (O_2) is finite as well. Since J_{ij}, and hence, the off-diagonal order parameter are present only for the nearest neighbors, we will define $\langle b_{i,i+\alpha}\rangle = \Delta_\alpha$ ($\alpha=x$ or y). In terms of Δ_α and $\sum_s \langle f_{is}^{\dagger} f_{js}\rangle \equiv \langle \chi_{ij}\rangle$, the mean-field free energy, F, based on the uniform and singlet RVB states is given as follows,

$$F=-2T\sum_k \ln\left[2\cosh\frac{E_k}{2T}\right] + T\sum_k \ln\left(1-\mathrm{e}^{-\omega_k/T}\right) + N\left[4\sum_\tau t_{0,\tau}\langle b_0 b_\tau^{\dagger}\rangle\langle \chi_{0,\tau}\rangle + \frac{3J}{4}|\langle \chi_{ij}\rangle|^2 + \frac{3J}{4}(|\Delta_x|^2+|\Delta_y|^2) - \mu\right]. \tag{2.2}$$

Here N is the total number of lattice sites, $E_k=\sqrt{\xi_k^2+|\Delta_k|^2}$ with

$$\xi_k=-2[F_1\gamma_k^{(1)}+F_2\gamma_k^{(2)}+F_3\gamma_k^{(3)}]-\mu, \tag{2.3}$$

$$\Delta_k=-\frac{3J}{2\sqrt{2}}(\Delta_x\cos k_x+\Delta_y\cos k_y), \tag{2.4}$$

and

$$\omega_k=-2[B_1\gamma_k^{(1)}+B_2\gamma_k^{(2)}+B_3\gamma_k^{(3)}]-\lambda, \tag{2.5}$$

with the chemical potentials, μ and λ. Here F_l's, B_l's, and $\gamma_k^{(l)}$'s are defined by $F_l=F_{ij}\equiv t_{ij}\langle b_i b_j^{\dagger}\rangle+(3/8)J_{ij}\langle \chi_{ij}\rangle$, $B_l=B_{ij}\equiv t_{ij}\langle \chi_{ij}\rangle$ for the l-th neighbour pairs (i,j), and $\gamma_k^{(l)}=(1/2)\sum_\tau \mathrm{e}^{ik\cdot\tau}$ where the summation is taken over the l-th nearest neighbor sites τ, i.e.,

$$\gamma_k^{(1)}=\cos k_x+\cos k_y, \tag{2.6a}$$

$$\gamma_k^{(2)}=2\cos k_x\cos k_y, \tag{2.6b}$$

$$\gamma_k^{(3)}=\cos 2k_x+\cos 2k_y. \tag{2.6c}$$

The mean-field self-consistent equations are given by

$$\langle \chi_{ij}\rangle^{(l)}=-\frac{1}{2N}\sum_k \frac{\gamma_k^{(l)}\xi_k}{E_k}\tanh\frac{E_k}{2T}, \tag{2.7}$$

$$\langle b_i b_j^{\dagger}\rangle^{(l)}=\frac{1}{2N}\sum_k \frac{\gamma_k^{(l)}}{\mathrm{e}^{\omega_k/T}-1}, \tag{2.8}$$

$$\Delta_\alpha=-\frac{1}{2N}\sum_k \cos k_\alpha\frac{\Delta_k}{E_k}\tanh\frac{E_k}{2T}, \tag{2.9}$$

$$\delta=\frac{1}{N}\sum_k\frac{\xi_k}{E_k}\tanh\frac{E_k}{2T} \tag{2.10}$$

$$=\frac{1}{N}\sum_k\frac{1}{\mathrm{e}^{\omega_k/T}-1}, \tag{2.11}$$

where the superscript (l) on $\langle \chi_{ij}\rangle$ and $\langle b_i b_j^{\dagger}\rangle$ in eqs. (2.7) and (2.8) means that i and j are the l-th nearest neighbor sites each other and δ is the hole-doping rate. Equations (2.10) and (2.11) determine the chemical potentials, μ and λ. The contribution of the $J\boldsymbol{S}_i\cdot\boldsymbol{S}_j$-term to F_{ij}, i.e., $(3/8)J_{ij}\langle \chi_{ij}\rangle$, follows from the decoupling,

$$\boldsymbol{S}_i\cdot\boldsymbol{S}_j=(1/4)\sum_{\alpha\beta\gamma\delta}(f_{i\alpha}^{\dagger}\sigma_{\alpha\beta}f_{i\beta})\cdot(f_{j\gamma}^{\dagger}\sigma_{\gamma\delta}f_{j\delta}) \rightarrow -(3/8)\{[\langle \chi_{ij}^{\dagger}\rangle\chi_{ij}+2\langle b_{ij}^{\dagger}\rangle b_{ij}+\mathrm{h.c.}] - [|\langle \chi_{ij}\rangle|^2+2|\langle b_{ij}\rangle|^2]\}, \tag{2.12}$$

which respects the SU(2) symmetry[47] at half filling. In our earlier study,[7] the term $\boldsymbol{S}_i\cdot\boldsymbol{S}_j$ has

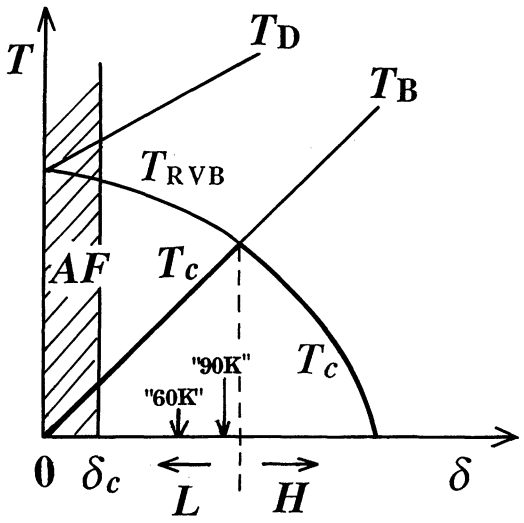

Fig. 3. A schematic representation of the mean-field phase diagram of the (extended) t-J model in the plane of the doping rate, δ, and the temperature, T; T_D, T_{RVB} and T_B are onset temperatures of the uniform RVB (coherent motions of spinons and holons), the singlet RVB pairing and the Bose condensation of holons, respectively. The arrows with "60 K" and "90 K" are the locations in our classification of T_c=60 K and T_c=90 K YBCO systems. (According to Horvatić *et al.*,[19] a so-called 90 K sample can be either in L or H in a closer look.)

been approximated as $-\chi_{ij}^{\dagger}\chi_{ij}/2$ leading to $F_{ij}=t_{ij}\langle b_i b_j^{\dagger}\rangle+(J/2)\langle\chi_{ij}\rangle$, and therefore, this symmetry has not been maintained.

The mean-field phase diagram is schematically shown in Fig. 3, where T_D, T_{RVB} and T_B are onset temperatures of coherent motion of holons and spinons, singlet pairing of spinons, and Bose condensation of holons (here, weak three-dimensionality is assumed), respectively. Even though these are sharp critical temperatures in the mean-field approximation, the fluctuations around it are shown to make the lower one between T_{RVB} and T_B true critical temperature,[48] which is the one of the onset of superconductivity. (In Fig. 3, the locations of T_c=60 K and T_c=90 K YBCO systems are indicated by arrows with "60 K" and "90 K", respectively, according to the present classification as illustrated in Fig. 1.)

We have solved eqs. (2.7), (2.9) and (2.10) under the assumption that holons are bose-condensed. This will not be so serious for the present study of magnetic properties which are governed by spinons and if the temperature is low compared with $T_D=T_D^{(0)}[1+\sqrt{1+2(t/T_D^{(0)})^2\delta/(1-\delta)}](1-\delta^2)/2$,[45] where $T_D^{(0)}=3J/16$ denotes T_D at $\delta=0$.

In the uniform RVB state without the singlet RVB, the energy spectra of spinons and holons are those of independent particles. Especially the spinons have the Fermi surface, which is shown in Fig. 4 for several choices of t'/t, t''/t and the doping rate, δ; Fig. 4(a) shows those in the ideal t-J model with transfer integral only between nearest neighbors, while parameters in Figs. 4(b) and 4(c) are chosen to reproduce the qualitative features of those in LSCO[30,31] and YBCO[32] concluded from LDA band calculations, which are essentially rotated by 45° relatively. The latter Fermi surface is consistent with that probed by the angle-resolved photoemission spectroscopy.[28] (In the uniform RVB state, the Fermi surfaces of electrons are the same as those of spinons but the life-time of quasiparticle near the Fermi energy is reduced by the gauge fields.) The similar LDA calculations for $Nd_{2-x}Ce_xCuO_4$,[33] $YBa_2Cu_4O_8$,[34] $Bi_2Sr_2CaCu_2O_8$,[35,36] $Tl_2Ba_2CaCu_2O_8$ and $Tl_2Ba_2Ca_2Cu_3O_{10}$[37] lead to the Fermi surfaces, which are basically the same as those in YBCO, and hence two different types shown in Figs. 4(b) and 4(c) can be considered to represent the typical cases of high-T_c cuprates. (Small pockets located around the middle of ΓZ [around Γ and Z] in the Bi-compounds [Tl-compounds] are due to Bi–O [Tl–O] bands, and hence are not essentially related to CuO_2 planes.) It is quite interesting to clarify the origin of the difference in the shape of the Fermi surface between LSCO- and YBCO-type systems.

There remains some arbitrariness in the choice of t'/t and t''/t, because we have chosen them rather arbitrarily to reproduce the shapes of the actual Fermi surfaces on the phenomenological ground. For example, the choice of $t'/t=-1/2$, $t''/t=0$ leads to the Fermi surfaces shown in Fig. 4(d), which are quite similar to those shown in Fig. 4(c) and cannot be excluded in the present approach. However, it seems that such a large value of t'/t is unrealistic and we rather favor to introduce the third neighbor hopping t'' which enables us to fit the Fermi surface with realis-

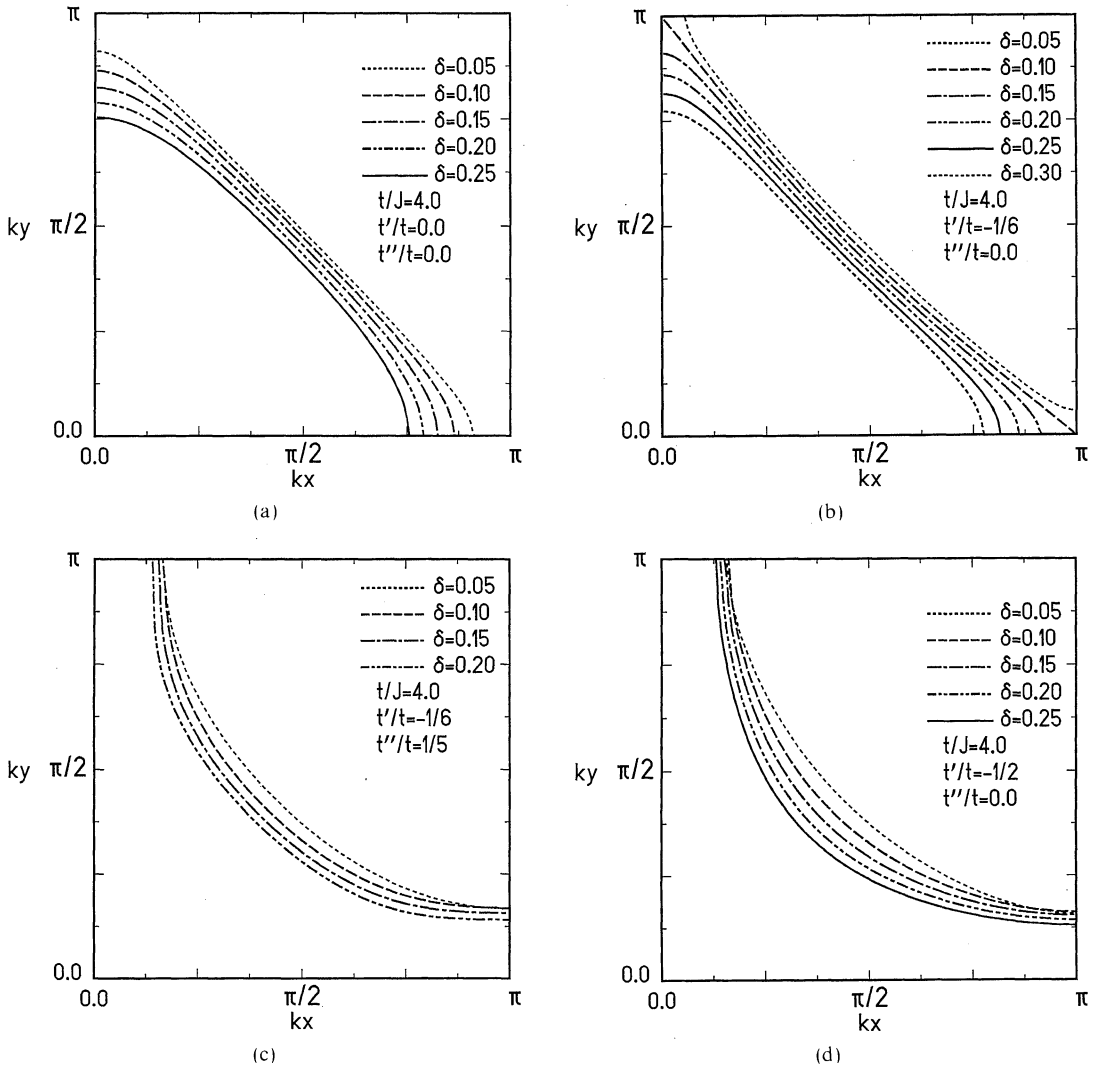

Fig. 4. The Fermi surfaces in the uniform RVB state of the extended t-J model for several doping rates; (a) $t'=t''=0$ (t-J model), (b) $t'/t=-1/6$, $t''/t=0$ (LSCO-type), (c) $t'/t=-1/6$, $t''/t=1/5$ (YBCO-type), (d) $t'/t=-1/2$, $t''/t=0$.

tic values of t'/t and t''/t. Possible microscopic reasonings behind these are left for the future study. Here we note that the spatial extent of the Zhang-Rice singlet, which determines the effective transfer integrals, is very sensitive to the parameters in the original d-p model including the location of the apical oxygens.[41]

In the following sections, we examine the magnetic properties of the extended t-J model on the basis of the RPA dynamical spin susceptibility, $\chi(\boldsymbol{q}, \omega)$, given by

$$\chi(\boldsymbol{q}, \omega)=\frac{\chi_0(\boldsymbol{q}, \omega)}{1+J_q\chi_0(\boldsymbol{q}, \omega)}, \tag{2.13}$$

where $J_q=J(\cos q_x+\cos q_y)$ and $\chi_0(\boldsymbol{q}, \omega)$ is that of independent spinons either in the uniform or singlet RVB state.

§3. Static Susceptibility in the Uniform RVB State

We first study the static susceptibility $\chi(\boldsymbol{q}, 0)$ in the uniform RVB state (i.e., $\Delta_\alpha=0$) for LSCO-type [Fig. 4(b)] and YBCO-type [Fig.

4(c)] Fermi surfaces. The case for Fig. 4(a) has been examined before.[7]

In Figs. 5(a, b) and 6(a, b) are shown $\chi_0(q, 0)\equiv\chi_0(q)$ and $\chi(q, 0)\equiv\chi(q)$ at low temperature along the symmetry axis for a choice of parameters leading to the Fermi surface of LSCO-type and YBCO-type, respectively. Their temperature dependences are shown in Fig. 7 for LSCO-type ($\delta=0.20$) and in Fig. 8 for YBCO-type ($\delta=0.15$), respectively. In each case the paramagnetic state gets unstable at some particular wave vector below some critical concentration, δ_c, whose dependences at absolute zero on either t' or t'' are shown in Figs. 9(a) and 9(b).

By comparing Figs. 5(b) and 6(b), we see that the sharp incommensurate (IC) peaks are present for the Fermi surface of Fig. 4(b) (LSCO-type) while rather broad commensurate (C) peaks exist in the case of Fig. 4(c) (YBCO-type). The reason for such a difference is the following;

(1) In LSCO-type Fermi surface, the nesting is present at wave vectors around $\boldsymbol{Q}$ where J_q is negative with large absolute magnitude. Hence the variation with respect to $\boldsymbol{q}$ is mainly governed by that of $\chi_0(q)$. In this case, the location in the q-space and the sharpness of IC-peaks are strongly dependent on temperature as has been found in TKF. Typical examples disclosing this interesting T-dependences are shown in Fig. 7 for $\delta=0.20$, which clearly shows the rapid suppression and the shift of IC peaks to the commensurate wave vector as the temperature is raised.

(2) In YBCO-type Fermi surface, $\chi_0(q)$ is

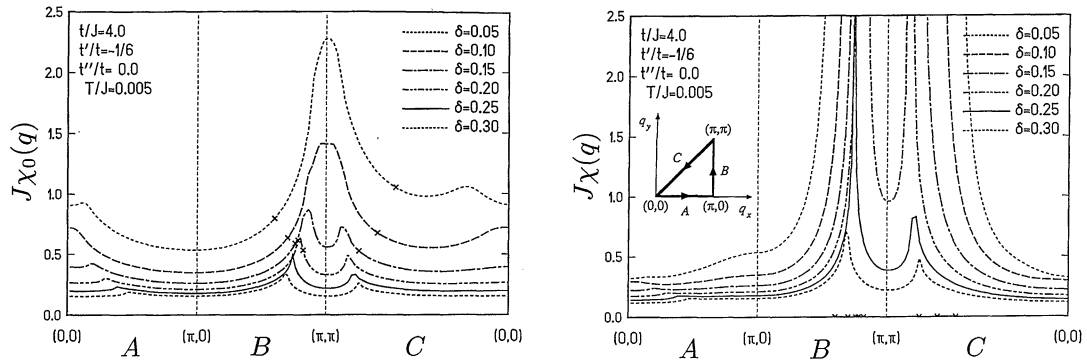

Fig. 5. The q-dependences of the static ($\omega=0$) spin susceptibility in the uniform RVB state for several choices of the doping rate in the case of $t'/t=-1/6$, $t''/t=0$ (LSCO-type); (a) $\chi_0(q)$, (b) $\chi(q)$.

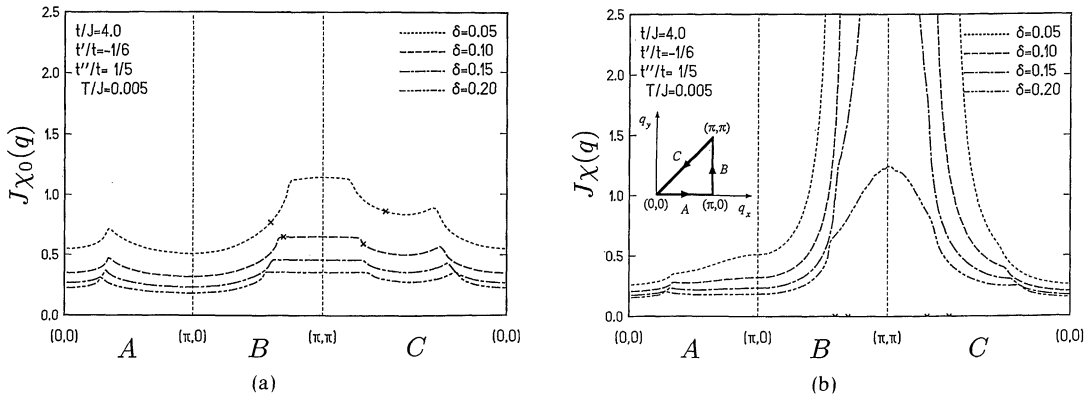

Fig. 6. The q-dependences of the static ($\omega=0$) spin susceptibility in the uniform RVB state for several choices of the doping rate in the case of $t'/t=-1/6$, $t''/t=1/5$ (YBCO-type); (a) $\chi_0(q)$, (b) $\chi(q)$.

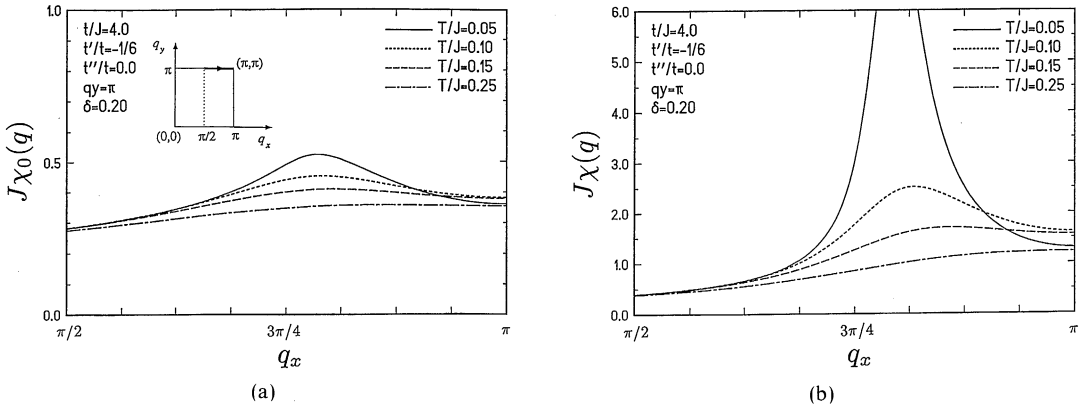

Fig. 7. The q-dependences of the static spin susceptibility in the uniform RVB state for several choices of temperature in the case of $t'/t=-1/6$, $t''/t=0$ (LSCO-type) with $\delta=0.20$; (a) $\chi_0(q)$, (b) $\chi(q)$.

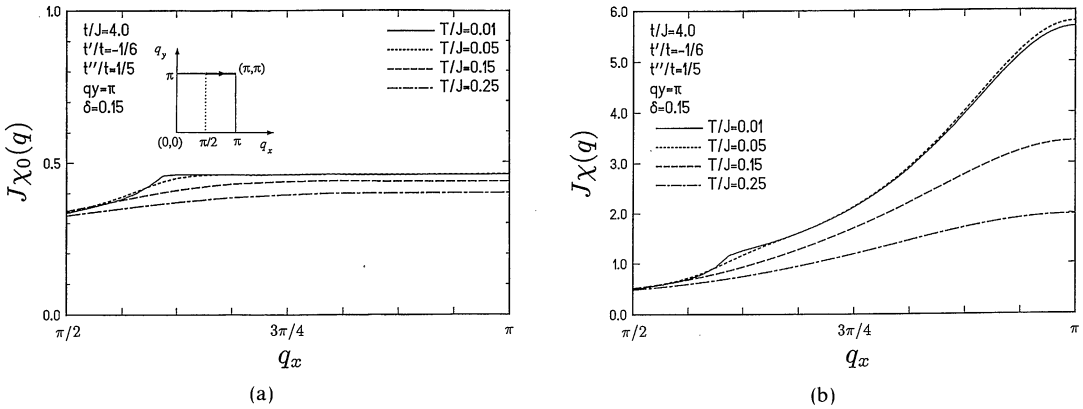

Fig. 8. The q-dependences of the static spin susceptibility in the uniform RVB state for several choices of temperature in the case of $t'/t=-1/6$, $t''/t=1/5$ (YBCO-type) with $\delta=0.15$; (a) $\chi_0(q)$, (b) $\chi(q)$.

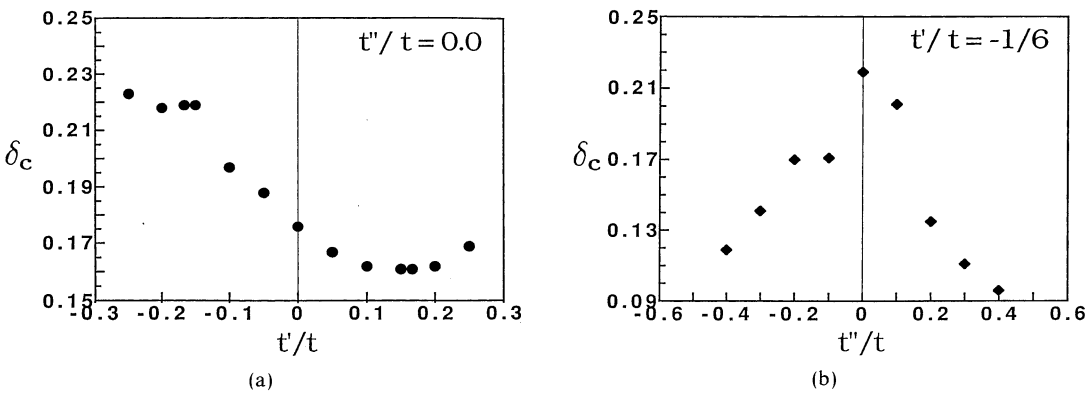

Fig. 9. The (a) t'/t- and (b) t''/t-dependences of the critical concentration, δ_c, of the magnetic instability of the uniform RVB state.

more or less constant in the whole Brillouin zone and the nesting effect is hardly seen. Hence the C-peak is mainly due to the q-dependence of J_q and the width in the q-space of the

C-peak is governed by $(\cos q_x+\cos q_y)$ resulting in a rather broad one.

The doping dependence of the location of the IC-peak, which is parametrized by η as $(\pi-\eta, \pi)$ or $(\pi, \pi-\eta)$, at absolute zero are shown in Fig. 10 for the t-J model and the LSCO-type model. Note, however, that the paramagnetic state we start with gets unstable for $\delta \lesssim 0.22$ (LSCO-type) or $\delta \lesssim 0.175$ (t-J model).

For the LSCO-type model, the temperature dependences of the IC-peak height, $\chi_{\max}$, its location parametrized by η as $(\pi, \pi-\eta)$ or $(\pi-\eta, \pi)$ as well as $\chi(\boldsymbol{Q})$ are shown in Fig. 11, both for $T>T_{\mathrm{RVB}}$ and $T<T_{\mathrm{RVB}}$.

For the YBCO-type model, the temperature dependences of the C-peak height, $\chi_{\max}$, and its width (defined as the half width in the q-space at half of the peak value), κ, are shown in Fig. 12, both for $T>T_{\mathrm{RVB}}$ and $T<T_{\mathrm{RVB}}$.

In the phenomenological approaches to spin fluctuations in high-T_c cuprates,[49-51] the spin susceptibility has often been modeled by such expressions like

$$\chi(\boldsymbol{Q}+\boldsymbol{q}, \omega=0)=\frac{\bar{\chi}}{\xi_0^2(\kappa^2+q^2)}, \tag{3.1}$$

$$\mathrm{Im}\,\chi(\boldsymbol{Q}+\boldsymbol{q}, \omega)=\bar{\chi}\frac{\pi\omega/\bar{\Gamma}}{\xi_0^4(\kappa^2+q^2)^2+(\pi\omega/\bar{\Gamma})^2}, \tag{3.2}$$

with the inverse correlation length, κ (and some constants, $\bar{\chi}$, ξ_0, and $\bar{\Gamma}$, with dimensions of inverse energy, length, and energy, respectively), which assumes that the peak is always located at $\boldsymbol{Q}$. While eq. (3.1) well describes that of YBCO near $\boldsymbol{q}=\boldsymbol{Q}$, it can hardly describe that of LSCO.

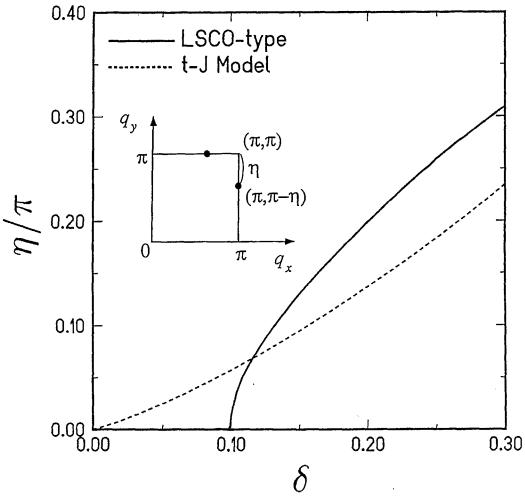

Fig. 10. The doping dependence of the location of the IC-peak parametrized by η as $(\pi-\eta, \pi)$ or $(\pi, \pi-\eta)$ at $T=0$, for the t-J model (dashed line) and the LSCO-type extended model (solid line).

These results, (1) and (2), share common features with those by Si *et al.*,[52] who employed the slave-boson technique to the d-p model. Recent numerical calculations on the Hubbard model also indicate that the strong incommen-

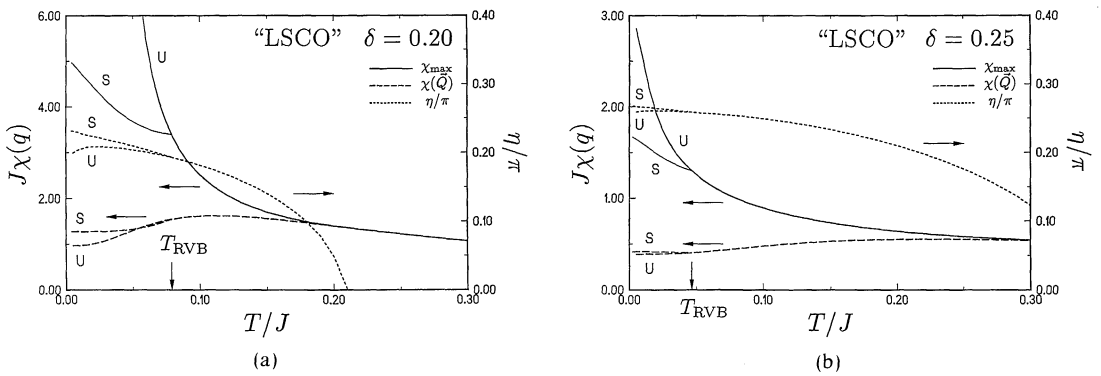

Fig. 11. The temperature dependences of the IC-peak height, $\chi_{\max}$, (solid line), its location, η, (dotted line) parametrized as $(\pi, \pi-\eta)$ and $\chi(\boldsymbol{Q})$ (dashed line) for $t'/t=-1/6$, $t''/t=0$ (LSCO-type). Below T_{RVB}, the line with a letter U indicates that in the uniform RVB state, whereas that with a letter S refers to that in the singlet RVB state. (a) $\delta=0.20$, (b) $\delta=0.25$. For the case of $\delta=0.20$, the uniform RVB state has magnetic instability below $T=0.0337J$.

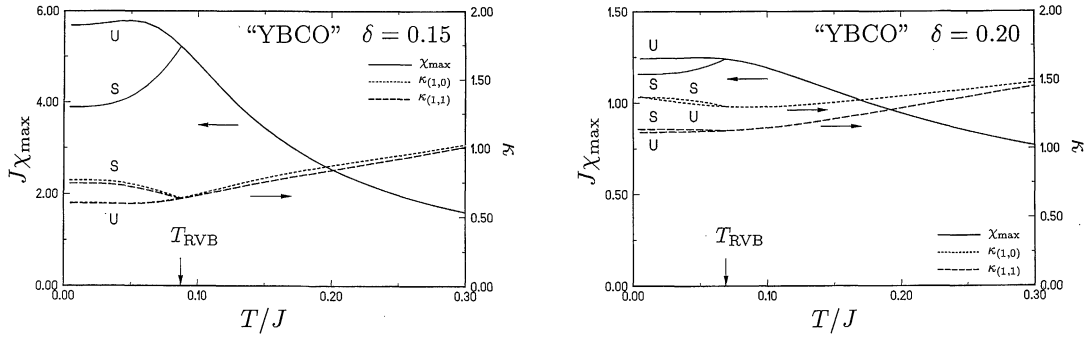

Fig. 12. The temperature dependences of the C-peak height, χ_{max}, (solid line), its half width (HWHM), $\kappa_{(1,0)}$, (dotted line) along the $(\pi, 0)$-(π, π) line and HWHM, $\kappa_{(1,1)}$, (dashed line) along the $(0, 0)$-(π, π) line for $t'/t=-1/6$, $t''/t=1/5$ (YBCO-type). Below T_{RVB}, the line with a letter U indicates that in the uniform RVB state, whereas that with a letter S refers to that in the singlet RVB state. (a) $\delta=0.15$, (b) $\delta=0.20$.

surate spin fluctuations are transformed into less sharp commensurate ones in the presence of t'.[53]

§4. Static Susceptibility in the Singlet RVB State

In this section the effects of the singlet formation are studied. We note that the d-symmetry ($\Delta_x=-\Delta_y$) is known to be most favorable[46] and then we confine ourselves to this case in the following. First the δ-dependences of the onset temperature, T_{RVB}, of the singlet RVB are shown in Fig. 13 for the cases of the ideal t-J model, LSCO- and YBCO-type models. Owing to the SU(2) symmetry, $T_{RVB}=3J/16$ $(=T_D)$ at half filling, $\delta=0$. (Here the onset of the antiferromagnetism at higher temperatures, which has been examined elsewhere,[54] has not been taken into account in the region of low doping.) It is seen that T_{RVB} for YBCO-type remains appreciable even in relatively high doping regime in contrast to that for LSCO-type.

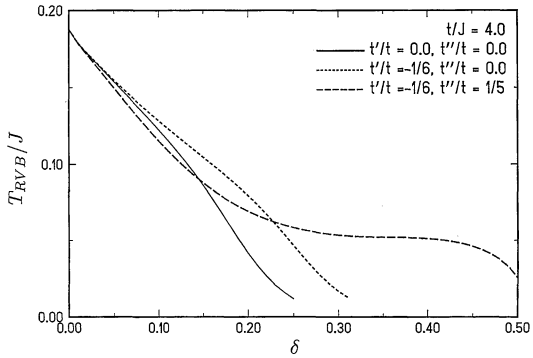

Fig. 13. The δ-dependences of T_{RVB} for several choices of t'/t and t''/t.

The q-dependences of $\chi_0(q)$ and $\chi(q)$ in the singlet RVB state are shown in Figs. 14(a, b) and 15(a, b) for LSCO and YBCO types, respectively, for several choices of temperature. As the temperature is lowered below T_{RVB}, IC-peaks in LSCO continue to sharpen, while C-peak in YBCO is appreciably suppressed. These will be consistent with neutron scattering by Thurston *et al.*[24] (LSCO) and Rossat-Mignod *et al.*[25] (YBCO) on samples with the optimal T_c, where the onset of the superconductivity will be characterized by that of the singlet RVB. It is interesting to see that the temperature dependences of $\chi(q)$ both at $q=0$, probed as the shift, K, of NMR, and at around $q=Q$ are strong while those near $(\pi, 0)$ are very weak. This feature is specific to the $(\cos k_x-\cos k_y)$-type d-wave pairing.[55]

The temperature dependences of $\chi(q)$ at $q=0$ for LSCO and YBCO types are shown in Figs. 16(a) and 16(b). The arrows denote T_{RVB}. In the present scenario, superconductivity in L-region sets in at T_B in Fig. 3, which is located anywhere below T_{RVB}, while it sets in at T_{RVB} in the H-region. Consequently, the Knight shift, K, is strongly dependent on temperature even above T_c in YBCO 60 K (L-region) but is constant down to T_c in YBCO

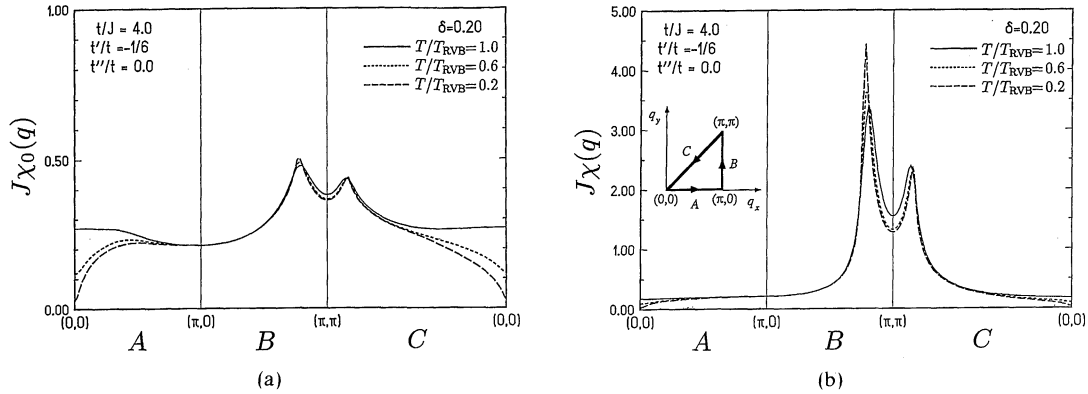

Fig. 14. The q-dependences of the static spin susceptibility in the singlet RVB state at several temperatures in the case of $t'/t=-1/6$, $t''/t=0$ (LSCO-type) with $\delta=0.20$ where $T_{\mathrm{RVB}}/J=0.0791$; (a) $\chi_0(q)$, (b) $\chi(q)$.

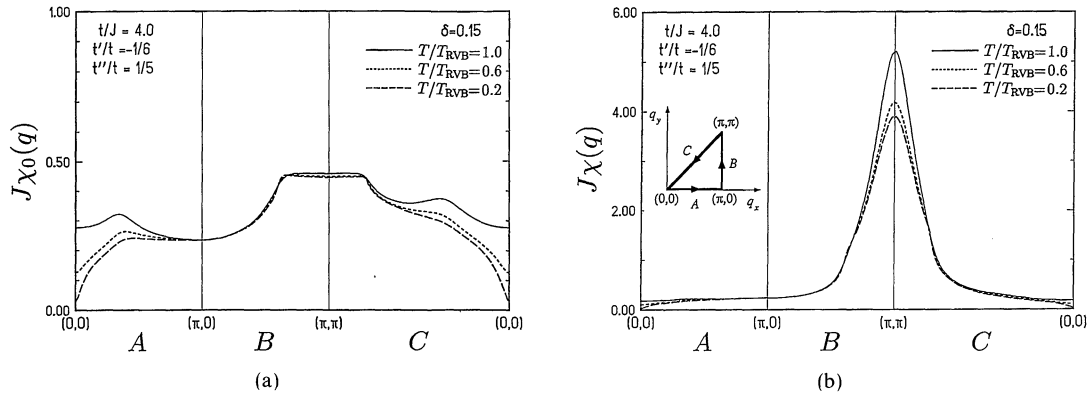

Fig. 15. The q-dependences of the static spin susceptibility in the singlet RVB state at several temperatures in the case of $t'/t=-1/6$, $t''/t=1/5$ (YBCO-type) with $\delta=0.15$ where $T_{\mathrm{RVB}}/J=0.0875$; (a) $\chi_0(q)$, (b) $\chi(q)$.

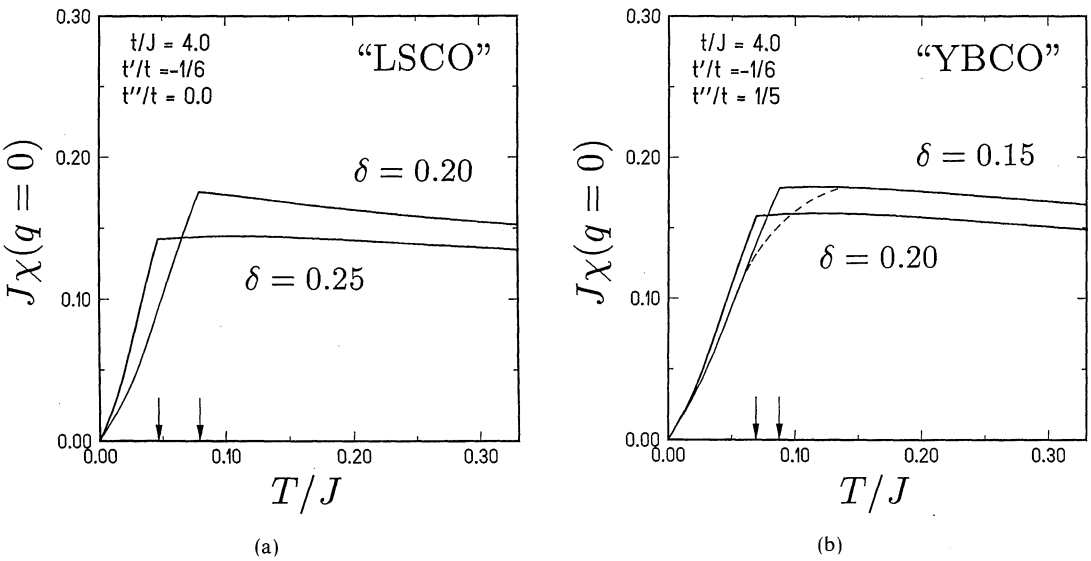

Fig. 16. The temperature dependences of $\chi(q=0)$ in the case of (a) $t'/t=-1/6$, $t''/t=0$ (LSCO-type), $\delta=0.20$, and (b) $t'/t=-1/6$, $t''/t=1/5$ (YBCO-type), $\delta=0.15$. The arrows indicate T_{RVB}.

90 K (H-region). In the L-region, T_{RVB} is only a crossover temperature if gauge fluctuations are taken into account,[48] and hence K will not have a sharp cusp at this temperature, but will start to decrease below around this temperature, as schematically shown by the dashed line in Fig. 16 for $\delta=0.15$ YBCO. These features are in qualitatively agreement with the experimental results.[11-13]

§5. Transverse Relaxation Time

The nuclear spin-spin relaxation rate, T_{G}^{-1}, due to the coupling mediated by conduction-electron polarization is given by[56,57]

$$T_{\mathrm{G}}^{-2}=\frac{C}{N}\sum_{q}[F(q)\chi(q)]^2, \tag{5.1}$$

where $F(q)$ is the form factor of hyperfine coupling. The constant C is given by 0.69/32 for ^{63}Cu nucleus, 0.69 being natural-abundance fraction of the ^{63}Cu isotope. The temperature dependences of T_{G}^{-1} at Cu sites of LSCO and YBCO through T_{RVB} are shown in Figs. 17(a) and 17(b), respectively, where we have normalized them by setting $C=1$ and $F(q)=[1-(\cos q_x+\cos q_y)/2]^2$. They approximately reflect the behaviours of $\chi(q)$ near $q=Q$; as the temperature is lowered, they increase in the uniform RVB state whereas they decrease in the singlet RVB state. It is also seen that there are no qualitative differences between LSCO and YBCO.

§6. Summary and Discussion

In this paper, we have extended the original t-J model to include the transfer integrals of extended range and thereby examined the effects of the shape of the Fermi surface on static magnetic properties. We have taken into account the singlet RVB order parameters in our calculations. This is because, as has been indicated in refs. 8 and 9, high-T_{c} cuprates seem to be classified into either high (H)- or low (L)-doping region depending on the temperature dependences of the shift (K) and the rate ($R=(T_1T)^{-1}$) of NMR on one hand, and this classification is apparently consistent with the results of the mean field theory[45] based on not only uniform but also singlet RVB states on the other hand.

The different shapes of the Fermi surface have led to the different structures of spin fluctuations near $q=Q\equiv(\pi,\pi)$, i.e., IC-peaks for the LSCO-type Fermi surface and C-peak for the YBCO-type Fermi surface. These features are consistent with neutron scattering experiments although more detailed comparison with experiments should be made by calculating Im $\chi(q,\omega)$ for finite ω, which will be discussed in a forthcoming paper.

NMR measurements had revealed the qualitative difference in spin fluctuations in normal phase depending on the doping regions; H or L, as illustrated in Fig. 1. In H-region, the Knight shift is almost independent

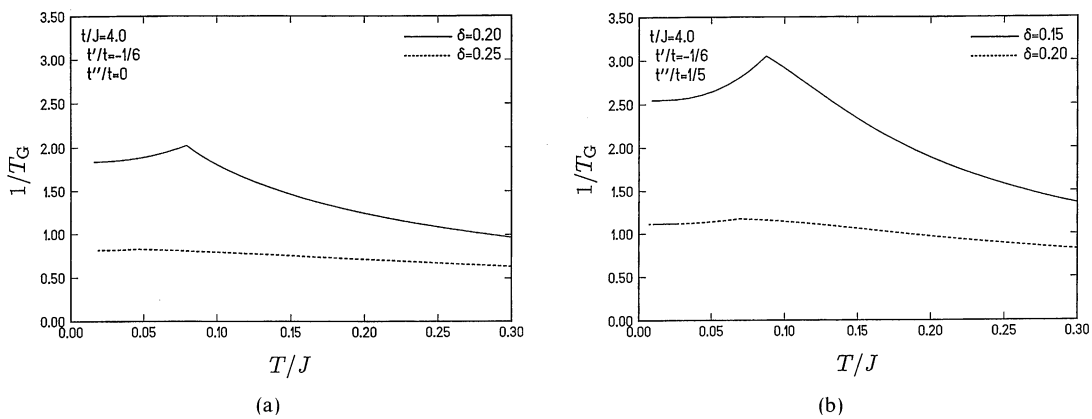

Fig. 17. The temperature dependence of transverse (Gaussian) relaxation rate, T_{G}^{-1}, of NMR. (a) $t'/t=-1/6$, $t''/t=0$ (LSCO-type), (b) $t'/t=-1/6$, $t''/t=1/5$ (YBCO-type).

of temperature whereas NMR rates, R and T_G^{-1}, increase with decreasing temperature (with a maximum in R). These behaviours are consistent with those calculated in the uniform RVB state.[7] On the other hand, in L-region, the Knight shift decreases as the temperature is lowered below T_S, which is well above the superconducting T_c, while R and T_G^{-1} continues to increase through T_S (with a maximum in R at $T=T_R<T_S$). This temperature dependence of the shift is consistent with the present calculation if the singlet RVB order parameter is taken into account and if the crossover temperature T_{RVB} is identified with T_S, as shown in Figs. 16(a) and 16(b). We note, however, that theoretical values of T_{RVB} shown in Fig. 13 are relatively low in comparison with experimental results, at least in YBCO, although it will be more or less in accordance with Nd–Ce–Cu–O and LSCO. One possible reason for this is the different degrees of coupling to the lattice distortions,[58] which may be related to the apparent absence of high T_c in the tetragonal phase.[59]

As regards T_G^{-1}, the present calculations predict its suppression as the temperature is lowered through T_{RVB}, while the experimental data in $YBa_2Cu_4O_8$,[60] which belongs to L-region in the present classification as deduced from the Knight shift measurements,[61] indicates that it continues to increase down to T_c; a clear contradiction. This experimental result implies that there is some range of temperature above T_c where the spin fluctuations, $\chi(q, 0)$, at $q=0$, probed by the shift, are suppressed while those at around $q=Q$, which contribute to T_G^{-1}, are enhanced as the temperature is lowered. In the present RVB mean field theory, however, as far as the static components ($\omega=0$) are concerned, both contributions $q=0$ and $q=Q$ are suppressed by the onset of the singlet pairing.

It will be important to check experimentally whether this discrepancy in the static ($\omega=0$) component of spin fluctuations is particular to $YBa_2Cu_4O_8$ or general, since the temperature dependence of T_G^{-1} is not the same as that of $(T_1T)^{-1}$ of NMR in this material, which is also governed by $q=Q$ components. This problem of identifying the characteristic features of $q=0$ and $q=Q$ components of the spin fluctuations is actually vital in the study of such dynamical properties as the rate of NMR, $(T_1T)^{-1}$, and the neutron scattering. This is being examined and will be reported in the forthcoming paper.

So far we have neglected the effect of the gauge-field fluctuations. It will not be so serious in discussing the qualitative aspects, although it can be important for quantitative discussions.[62]

In summary, we have carried out explicit calculations based on the extended t-J model in the slave-boson mean-field approximation. Although there are many problems which need further clarification, it is still encouraging to see the overall qualitative correspondence between the present calculation and the experimental results.

Acknowledgements

We thank H. Alloul, K. Asayama, C. Berthier, Y. Endoh, D. R. Grempel, M. Imada, Y. Kitaoka, M. Lavagna, H. Matsukawa, J. Rossat-Mignot, M. Sato, K. Terakura and H. Yasuoka for enlightening discussions. One of us (H. K.) also thanks Y. Itoh for instructive discussions. The present calculation has been performed by the Fujitsu FACOM M-380 system at the Institute for Solid State Physics, University of Tokyo. Various figures were drawn using a computer program written by T. Ando, to whom we thank. This work is supported by Monbusho International Scientific Research Program: Joint Research "Magnetism and Superconductivity in Highly Correlated Systems" (03044037) and Grant-in-Aid for Scientific Research on Priority Areas, "Science of High T_c Superconductivity" (04240103) of Ministry of Education, Science and Culture.

References

1) For various papers reported at M²S-HTSC III (Kanazawa, 1991) see Physica C **185–189** (1991).
2) *The Los Alamos Symposium—1989 High Temperature Superconductivity*, ed. K. S. Bedell, D. Coffey, D. E. Meltzer, D. Pines and J. R. Schrieffer (Addison-Wesley, 1990).
3) *Strong Correlation and Superconductivity*, ed. H. Fukuyama, S. Maekawa and A. P. Malozemoff (Springer-Verlag, 1989).
4) *The Physics and Chemistry of Oxide Superconduc-*

tors, ed. Y. Iye and H. Yasuoka (Springer Verlag, 1992).
5) For an overview, see M. Luchini, M. Ogata, W. Putikka and T. M. Rice: p. 141 of ref. 1.
6) N. Nagaosa and P. A. Lee: Phys. Rev. Lett. **64** (1990) 2450; P. A. Lee and N. Nagaosa: Phys. Rev. **B46** (1992) 5621.
7) T. Tanamoto, K. Kuboki and H. Fukuyama: J. Phys. Soc. Jpn. **60** (1991) 3072. In this paper (TKF), all energy scales should be halved except J appearing as the exchange correction factor. Therefore, δ_c, the critical hole-concentration for the instability of the paramagnetic state, has been estimated incorrectly. (The correct value is about factor two larger than that in TKF.) See also D. R. Grempel and M. Lavagna: preprint.
8) T. M. Rice: ref. 4, p. 313.
9) H. Fukuyama: Prog. Theor. Phys. Suppl. No. 108 (1992) 287; also in *Physics in (2+1)-Dimension*, ed. Y. M. Cho (World Scientific, 1992) p. 234.
10) H. Yasuoka, T. Imai and T. Shimizu: ref. 3, p. 254.
11) R. E. Walstedt, W. W. Warren, Jr., R. F. Bell, R. J. Cava, G. P. Espinosa, L. F. Schneemeyer and J. V. Waszczak: Phys. Rev. **B41** (1990) 9574.
12) M. Takigawa, A. P. Rayers, P. C. Hammel, J. D. Thomson, R. H. Heffner, Z. Fisk and K. C. Ott: Phys. Rev. **B43** (1991) 247.
13) H. Alloul, P. Mendels, H. Casalta, J.F. Marucco and J. Arabski: Phys. Rev. Lett. **67** (1991) 3140.
14) M. Takigawa, P. C. Hammel, R. H. Heffner and Z. Fisk: Phys. Rev. **B39** (1989) 7371.
15) Y. Kitaoka, K. Fujiwara, K. Ishida, K. Asayama, Y. Shimakawa, T. Manako and Y. Kubo: Physica C **179** (1991) 107.
16) S. Kambe, Y. Yoshinari, H. Yasuoka, A. Hayashi and Y. Ueda: ref. 4, p. 361.
17) R. E. Walstedt, R. F. Bell and D. B. Mitzi: Phys. Rev. **B44** (1991) 7760.
18) Y. Yoshinari, H. Yasuoka and Y. Ueda: J. Phys. Soc. Jpn. **61** (1992) 770.
19) M. Horvatić, C. Berthier, Y. Berthier, P. Butaud, W. G. Clark, J. A. Gillet, P. Ségransan and J. Y. Henry: preprint.
20) R. J. Birgeneau, Y. Endoh, K. Kakurai, Y. Hidaka, T. Murakami, M. A. Kastner, T. R. Thurston, G. Shirane and K. Yamada: Phys. Rev. **B39** (1989) 2868.
21) T. R. Thurston, R. J. Birgeneau, M. A. Kastner, N. W. Preyer, G. Shirane, Y. Fujii, K. Yamada, Y. Endoh, K. Kakurai, M. Matsuda, Y. Hidaka and T. Murakami: Phys. Rev. **B40** (1989) 4585.
22) G. Shirane, R. J. Birgeneau, Y. Endoh, P. Gehring, M. A. Kastner, K. Kitazawa, H. Kojima, I. Tanaka, T. R. Thurston and K. Yamada: Phys. Rev. Lett. **63** (1989) 330.
23) S. W. Cheong, G. Aeppli, T. E. Mason, H. Mook, S. M. Hayden, P. C. Canfield, Z. Fisk, K. N. Clausen and J. L. Martinez: Phys. Rev. Lett. **67** (1991) 1791.
24) T. R. Thurston, R. J. Birgeneau, Y. Endoh, P. M. Gehring, M. A. Kastner, H. Kojima, M. Matsuda, G. Shirane, I. Tanaka and K. Yamada: preprint.
25) J. Rossat-Mignod, L. P. Regnault, C. Vettier, P. Bourges, P. Burlet, J. Bossy, J. Y. Henry and G. Lapertot: Physica C **185–189** (1991) 86.
26) J. M. Tranquada, P. M. Gehring, G. Shirane, S. Shamoto and M. Sato: Phys. Rev. **B46** (1992) 5561.
27) M. Sato, S. Shamoto, T. Kiyokura, K. Kakurai, G. Shirane, J. M. Tranquada and P. M. Gehring: preprint.
28) J. C. Campuzano, G. Jennings, M. Faiz, L. Beaulaigue, B. W. Veal, J. Z. Liu, A. P. Paulikas, K. Vandervoort, H. Claus, R. S. List, A. J. Arko and R. J. Bartlett: Phys. Rev. Lett. **64** (1990) 2308.
29) C. G. Olson, R. Liu, D. W. Lynch, R. C. List, A. J. Arko, B. W. Veal, Y. C. Chang, P. Z. Jiang and A. P. Paulikas: Phys. Rev. **B42** (1990) 381.
30) L.F. Mattheiss: Phys. Rev. Lett. **58** (1987) 1028.
31) J.-H. Xu, T. J. Watson-Yang, J. Yu and A. J. Freeman: Phys. Lett. A **120** (1987) 489.
32) J. Yu, S. Massidda, A. J. Freeman and D. D. Koeling: Phys. Lett. A **122** (1987) 203.
33) S. Massidda, N. Hamada, J. Yu and A. J. Freeman: Physica C **157** (1989) 571.
34) T. Oguchi, T. Sasaki and K. Terakura: Physica C **172** (1990) 277.
35) S. Massidda, J. Yu and A. J. Freeman: Physica C **152** (1988) 251.
36) H. Krakauer and W. E. Pickett: Phys. Rev. Lett. **60** (1988) 1665.
37) J. Yu, S. Massidda and A. J. Freeman: Physica C **152** (1988) 273.
38) T. Tanamoto, K. Kohno and H. Fukuyama: J. Phys. Soc. Jpn. **61** (1992) 1886.
39) H. Matsukawa and H. Fukuyama: J. Phys. Soc. Jpn. **58** (1989) 3687.
40) L. H. Tjeng, H. Eskes and G. A. Sawatzky: p. 33 of ref. 3.
41) H. Matsukawa and H. Fukuyama: J. Phys. Soc. Jpn. **59** (1990) 1723.
42) F. C. Zhang and T. M. Rice: Phys. Rev. **B37** (1988) 3759.
43) P. W. Anderson: Science **235** (1987) 1196.
44) G. Baskaran, Z. Zou and P. W. Anderson: Solid State Commun. **63** (1987) 973.
45) Y. Suzumura, Y. Hasegawa and H. Fukuyama: J. Phys. Soc. Jpn. **57** (1988) 401, 2768; Physica C **153–155** (1988) 1630.
46) G. Kotliar and J. Liu: Phys. Rev. **B38** (1988) 5142.
47) I. Affleck, Z. Zou, T. Hsu and P. W. Anderson: Phys. Rev. **B38** (1988) 745.
48) N. Nagaosa and P. A. Lee: Phys. Rev. **B45** (1992) 966.
49) A. J. Millis, H. Monien and D. Pines: Phys. Rev. **B42** (1990) 167.
50) T. Moriya, Y. Takahashi and K. Ueda: J. Phys. Soc. Jpn. **59** (1990) 2905.
51) H. Kohno and K. Yamada: Prog. Theor. Phys. **85** (1991) 13.
52) Q. Si, Y. Zha, K. Levin, J. P. Lu, Ju. H. Kim: preprint.
53) N. Furukawa and M. Imada: J. Phys. Soc. Jpn. **61**

(1992) 3331.
54) H. Matsukawa and H. Fukuyama: J. Phys. Soc. Jpn. **61** (1992) 1882.
55) N. Bulut and D. J. Scalapino: Phys. Rev. B**45** (1992) 2371.
56) C. H. Pennington and C. P. Slichter: Phys. Rev. Lett. **66** (1991) 381.
57) N. Bulut and D. J. Scalapino: Phys. Rev. Lett. **67** (1991) 2898.
58) P. W. Anderson, G. Baskaran, Z. Zou and T. Hsu: Phys. Rev. Lett. **38** (1988) 745.
59) H. Takagi, R. J. Cava, M. Marezio, B. Batlogg, J. J. Krajewski, W. F. Peck, Jr., P. Bordet and D. E. Cox: Phys. Rev. Lett. **68** (1992) 3777.
60) Y. Itoh, H. Yasuoka, Y. Fujiwara, Y. Ueda, T. Machi, I. Tomeno, K. Tai, N. Koshizuka and S. Tanaka: J. Phys. Soc. Jpn. **61** (1992) 1287.
61) T. Machi, I. Tomeno, T. Miyatake, N. Koshizuka, S. Tanaka, T. Imai and H. Yasuoka: Physica C **173** (1991) 32.
62) H. Fukuyama and K. Kuboki: J. Phys. Soc. Jpn. **59** (1990) 2617.